Characterization and thermodynamic properties of quadruplex/duplex competition

Wei Li[a], Peng Wu[a], Tastuo Ohmichi[a], Naoki Sugimoto[a,b,*]

[a] *High Technology Research Center, Konan University, 8-9-1 Okamoto, Higashinada-ku, Kobe 658-8501, Japan*
[b] *Department of Chemistry, Faculty of Science and Engineering, Konan University, 8-9-1 Okamoto, Higashinada-ku, Kobe 658-8501, Japan*

Received 22 May 2002; accepted 15 July 2002

First published online 30 July 2002

Edited by Horst Feldmann

Abstract Structural characteristics and thermodynamic properties of $dG_3(T_2AG_3)_3$, $d(C_3TA_2)_3C_3$ and $dG_3(T_2AG_3)_3$/$d(C_3TA_2)_3C_3$ were intensively investigated. It was indicated that metal ions greatly affected the conformation and stability of the G-quadruplex. A competition of a structure transition among the G-quadruplex, I-motif, and the duplex was confirmed to be dependent on both cation species and pH values. The structural competitive mechanism is discussed for the first time. This study shows an intriguing potential in modulating DNA structures in vivo, which is of great importance in drug design and cancer chemotherapy.

Key words: G-quadruplex; I-motif; Structure competition; Duplex; Polycation

1. Introduction

Guanine/cytosine (G/C)-rich sequences are found to exist in biologically important regions of DNA, e.g. the end of chromosome telomere, immunoglobulin switch regions and the regulatory regions of oncogenes [1–3]. The tandemly repeated sequences, with three or four contiguous guanines, have been known to form polymorphic quadruplexes containing G-quartets stabilized by cyclic Hoogsteen hydrogen bondings [4,5]. C-rich oligomers have also been shown to self-associate at acidic or even neutral pH into an intercalated structure called the I-motif [6–8]. Recently, structures of synthetic oligonucleotides corresponding to either G-rich or C-rich strands have been investigated extensively because of their unusual aggregation properties and possible specialized biological functions [9–13]. G-rich sequences should form the stable duplex structures with their complementary C-rich sequences, according to the well-established Watson–Crick (WC) base pairs. However, there have appeared several reports that indicated some repetitive DNA sequences adopted unusual pairing arrangements with their relevant complements other than the WC pairing. Miura and Thomas [14] and Deng and Braunlin [15] reported that a B-form duplex DNA was able to interconvert to intermolecular G-quadruplex structures under certain cation concentrations. Additionally, Manzini et al. [16] observed that quadruplex structures were stable enough to postpone or prevent the formation of the WC duplex in an equimolar mixture of $dAG_3(T_2AG_3)_3$ and $d(C_3TA_2)_3C_3T$ at acidic pH. So far, few studies have been reported on the characteristics of structure transition competition between the WC duplex and quadruplex structures in a double-stranded system. This conformational information plays an important role in modulating the tertiary structures and understanding the biological activity of nucleic acids in vivo, which will be very useful for the design of structure-specific oligonucleotides for antigen chemotherapy.

In this article, conformational and thermodynamic properties of the human/vertebrate telomeric repeat oligonucleotides $dG_3(T_2AG_3)_3$ and $d(C_3TA_2)_3C_3$ were studied intensively using UV, circular dichroism (CD), differential scanning calorimetry (DSC) and polyacrylamide gel electrophoresis (PAGE) methods. All the results reflect the fact that a structure conversion competition among the duplex, G-quadruplex, and I-motif indeed exists in the double-stranded system of $dG_3(T_2AG_3)_3$/$d(C_3TA_2)_3C_3$, and the structural competitive equilibrium is proved to be dependent on both cation species and pH values. This is the first report on formation of an alternative structure to the WC duplex for the G-rich strand and its complementary sequence with equal length.

2. Materials and methods

2.1. Materials

21-mer DNA oligonucleotides, $dG_3(T_2AG_3)_3$, $d(C_3TA_2)_3C_3$, $dG_3(A_3G_3)_3$ and $d(C_3T_3)_3C_3$, were purchased from Espec Oligo Service Corp. (Japan). Oligonucleotides were purified by a reversed-phase high-performance liquid chromatography. Single-strand concentrations were determined by measuring the absorbance (260 nm) at high temperature. The different DNA strands were mixed in equimolar amounts and the total species concentrations were estimated by averaging the extinction coefficients of the single strands [17]. All measurements were performed in a buffer solution consisting of 50 mM MES at pH 7.0; the ionic strength was adjusted by the addition of the appropriate salt.

2.2. UV spectroscopy

UV thermal scans were carried out on Hitachi U-3200 and U-3210 spectrophotometers equipped with Hitachi SPR-10 thermoprogrammer and temperature probe. Water condensation on the cuvette exterior in the low-temperature range can be avoided by flushing with a constant stream of dry nitrogen. Melting curves were collected by UV absorbance as a function of temperature. The heating rates were fixed at 0.5 or 1.0°C/min according to the cuvette path lengths and strand concentrations. Prior to the sample experiments, all samples were annealed and degassed by heating the sample cuvette to 90°C for 10 min and then cooling to 0°C. The samples were allowed to stabilize

*Corresponding author. Fax: (81)-78-435 2539.
E-mail address: sugimoto@konan-u.ac.jp (N. Sugimoto).

0014-5793/02/$22.00
PII: S0014-5793(02)03118-6

for about 20 min at the beginning temperature of each heating–cooling cycle.

2.3. Circular dichroism

CD spectra were recorded on a Jasco J-820 spectropolarimeter equipped with a PTC-423L temperature controller. For each sample, at least four spectrum scans were accumulated over the wavelength range of 190–350 nm and the temperature range of 0–90°C in a 0.1 cm path length cell at a scanning rate of 20 nm/min. The scan of the buffer alone was subtracted from the average scan for each sample. CD spectra were collected in units of millidegrees versus wavelength and normalized to the total species concentrations. The cell holding chamber was flushed with a constant stream of dry nitrogen gas to avoid water condensation on the cell exterior.

2.4. Differential scanning calorimetry

DSC was performed on a MicroCal VP-DSC microcalorimeter. Prior to scanning, the buffer and the samples were vacuum-degassed. Buffer versus buffer cells were scanned to determine the baseline of the instrumental variation between the cells of the calorimeters before DNA samples versus buffer scans were collected. For each DNA sample, eight scans were collected from 5 to 95°C at a rate of 60°C/h. The resulting sample versus buffer scans collected for each sample were averaged, the buffer versus buffer baseline was subtracted, and then normalized by the strand concentration and sample volume to obtain the excess heat capacity.

2.5. Polyacrylamide gel electrophoresis

The oligonucleotide strands were 5′-end labeled with fluorenscein and annealed by heating the samples to 90°C for 5 min and cooling to 4°C for several hours. Native PAGE experiments were carried out using the fluorenscein-labeled oligonucleotides in 0.089 M Tris–borate buffers (pH 7.0) and 5 mM Tris–acetate buffers (pH 5.5), respectively. The same buffer was used in the polymerization of the acrylamide for the relevant gels. Electrophoresis was carried out using 20% total acrylamide (29:1 acrylamide: bis(acrylamide)) at 4 V/cm and 4°C.

3. Results and discussion

3.1. Cation effects on conformation of G-quadruplex

The conformational characteristics of $dG_3(T_2AG_3)_3$ were detected by CD spectra in the presence of monovalent (Na^+, K^+), divalent (Mg^{2+}), and polyamine (spermine, spermidine) cations, respectively. Fig. 1 indicated that CD profiles in both Na^+ and Mg^{2+} had a positive band at 295 nm and a negative band near 265 nm, which is typical of an antiparallel G-quadruplex structure [10]. Similar characteristic CD spectra were also observed for $dG_3(T_2AG_3)_3$ in buffers containing spermine (Sp^{4+}) and spermidine (Sp^{3+}), respectively (data not shown). On the other hand, in the presence of K^+ there

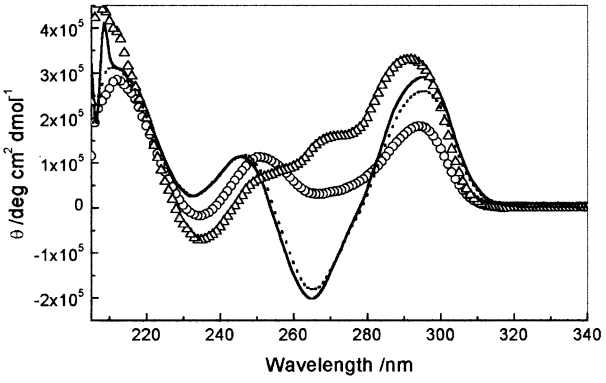

Fig. 1. CD spectra of $dG_3(T_2AG_3)_3$ in 50 mM MES buffer (pH 7.0) with 100 mM Na^+ (solid line), 100 mM K^+ (△), 10 mM Mg^{2+} (dotted line), and without cations (○), respectively. All spectra were collected at 0°C and in a strand concentration of 50 μM.

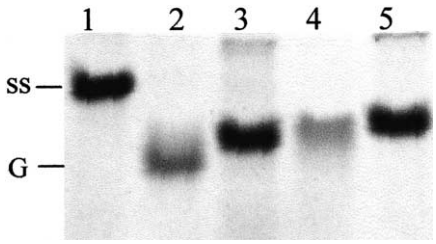

Fig. 2. Native PAGE images in 50 mM MES buffer (pH 7.0) with 100 mM K^+. Lane 1 contains $d(T)_{21}$ as a single-stranded marker. Lanes 2 and 3 contain $dG_3(T_2AG_3)_3$ and $d(C_3TA_2)_3C_3$, respectively. Lanes 4 and 5 contain $dG_3(A_3G_3)_3$ and $d(C_3T_3)_3C_3$, respectively.

appeared a small peak around 265 nm and a negative band near 240 nm, together with a stronger positive band at 295 nm. Generally, a peak near 270 nm and a negative band around 240 nm are ascribed to a parallel G-quadruplex structure [18]. Therefore, the conformation of $dG_3(T_2AG_3)_3$ with K^+ may be a mixture of parallel and anti-parallel G-quadruplex, although this needs to be ascertained by other experiments.

In both K^+ and Na^+ buffers, UV melting curves of $dG_3(T_2AG_3)_3$ showed no concentration dependence, and both of the melting profiles appeared as inverted-sigmoid shapes at 295 nm, whereas a sigmoid curve without clear upper baseline was obtained at 260 nm (data not shown). Further, we compared the electrophoretic mobility of $dG_3(T_2AG_3)_3$ in K^+ buffer with those in Na^+ and Mg^{2+} buffers through the native PAGE images. It is shown that $dG_3(T_2AG_3)_3$ had a much faster electrophoretic mobility than the single strand $d(T)_{21}$ in the presence of K^+, Na^+ or Mg^{2+} (as shown in Figs. 2 and 3). This fast mobility is concordant with a compact intramolecular G-quartet structure [19]. These PAGE images disproved the formation of a multi-stranded parallel G-quadruplex for $dG_3(T_2AG_3)_3$ in K^+ buffer.

Marathias and Bolton [20] suggested that there are two types of G-quartet structure formed by intramolecular fold-

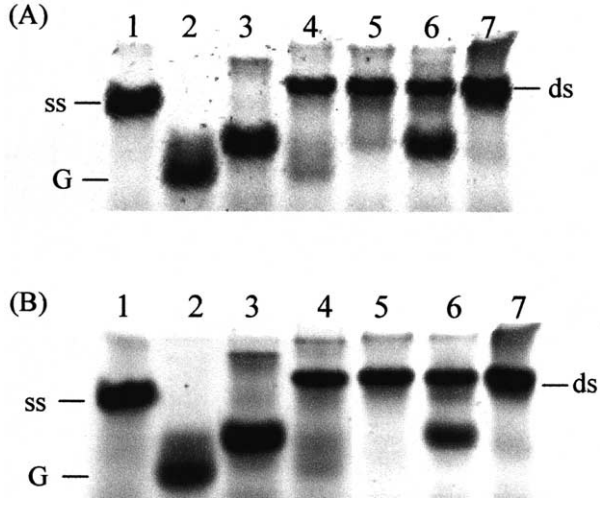

Fig. 3. Native PAGE images in 50 mM MES buffer (pH 7.0) with 100 mM Na^+ (A) and 10 mM Mg^{2+} (B), respectively. Lane 1 contains $d(T)_{21}$ as a single-stranded marker. Lanes 2 and 3 contain $dG_3(T_2AG_3)_3$ and $d(C_3TA_2)_3C_3$, respectively. Lanes 4–6 contain $dG_3(T_2AG_3)_3/d(C_3TA_2)_3C_3$ with a molar ratio of 2:1, 1:1 and 1:2, respectively. Lane 7 contains $d(T)_{21}/d(A)_{21}$ as a double-stranded marker. ss, single strand; G, G-quadruplex; ds, duplex.

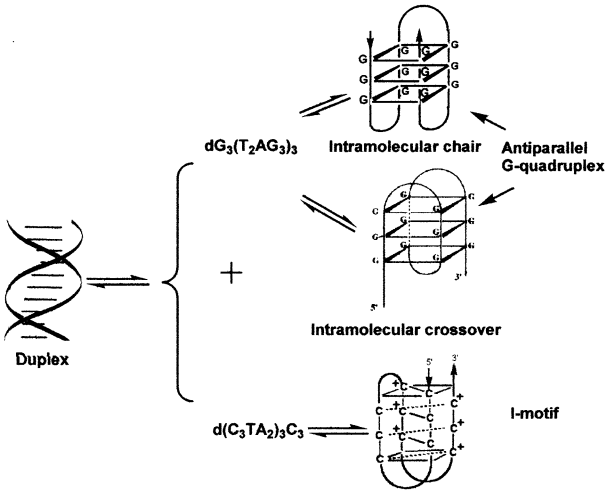

Scheme 1. Structural transition competition in $dG_3(T_2AG_3)_3$/$d(C_3TA_2)_3C_3$.

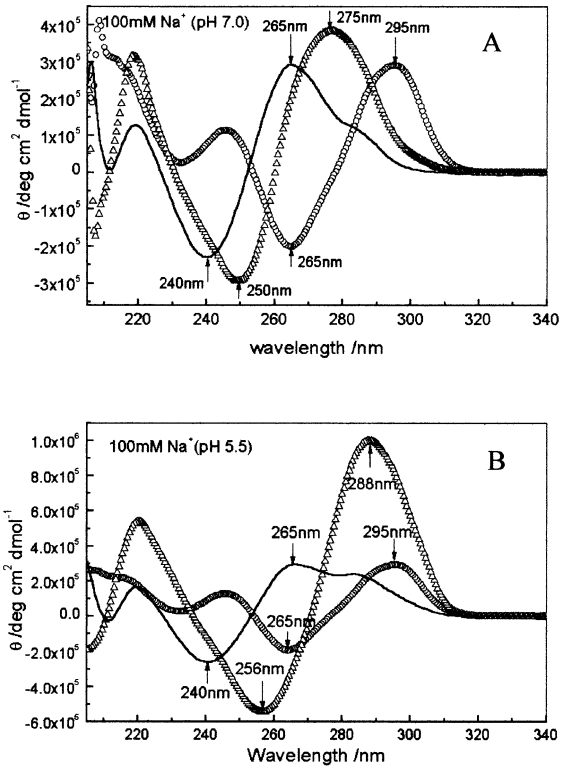

Fig. 4. CD spectra of $dG_3(T_2AG_3)_3$ (○), $d(C_3TA_2)_3C_3$ (△) and $dG_3(T_2AG_3)_3$/$d(C_3TA_2)_3C_3$ (—) in 100 mM Na^+ buffer (50 mM MES) at pH 7.0 (A) and pH 5.5 (B), respectively. All the spectra were collected at 0°C and in a species concentration of 50 μM.

ings, as depicted in Scheme 1, i.e. the crossover type and the chair type. The former type can be formed in the presence of sodium alone as well as in potassium, while the latter has only been observed in the presence of potassium. According to the above results we considered that the different CD spectra of $dG_3(T_2AG_3)_3$ with K^+ were attributed to a special K^+-induced chair-type quadruplex.

Stabilizing capacities of cations on $dG_3(T_2AG_3)_3$ can be compared through the thermodynamic parameters listed in Table 1, which were calculated from the CD melting curves at 295 nm using a non-linear least-squares fitting. The G-quartet structure was the most stable with monovalent cations but the least stable with Mg^{2+}. The G-quadruplex in K^+ was only marginally more stable than its counterpart in Na^+, with a difference in the free energy change at 37°C ($\Delta\Delta G_{37}$) of 1.7 kcal/mol. Balagurumoorthy and Brahmachari [21] reported that the difference of the free energy change at 25°C ($\Delta\Delta G_{25}$) between K^+- and Na^+-induced G-quadruplex was 2.7 kcal/mol for the four-copy human telomeric sequence $d(T_2AG_3)_4$. In our results, for the 3.5-copy human telomeric sequence $dG_3(T_2AG_3)_3$, the $\Delta\Delta G_{25}$ is 1.8 kcal/mol. The difference of the free energy change per G-quartet is consistent between these two model oligonucleotides.

3.2. Stability of I-motif

The conformation properties of the complementary C-rich sequence, $d(C_3TA_2)_3C_3$, were also investigated in this study. CD spectra of $d(C_3TA_2)_3C_3$ showed little dependence on the cation species (data not shown). In CD profiles with either Na^+ or K^+ a positive band around 275 nm and a negative one near 250 nm existed at neutral pH, whereas a peak near 288 nm and a trough near 256 nm appeared at pH 5.5 (as shown in Fig. 4). These bands in the CD spectra and their red-shift as the pH lowered to 5.5 are attributed to the I-motif structure and its pH-dependence, respectively [22]. UV melting curves of $d(C_3TA_2)_3C_3$ in 100 mM Na^+ showed a low transition temperature of 5.2°C at neutral pH versus 54°C at pH 5.5, without dependence on sequence concentrations. The electrophoretic mobility of $d(C_3TA_2)_3C_3$ was also faster than the single-strand marker (as shown in Fig. 2), which suggested that it formed an intramolecular folding structure. At pH 5.5 Na^+ buffer, the enthalpy, entropy and free energy change of $d(C_3TA_2)_3C_3$ were -79.3 ± 1.1 kcal/mol, -220 ± 3.3 cal/mol K and -11.1 ± 1.5 kcal/mol, respectively, calculated from its CD melting curves at 288 nm. This indicated that at acidic pH the I-motif structure was as stable as the G-quadruplex, compared with the data in Table 1.

Table 1
Thermodynamic parameters of antiparallel G-quadruplex of $dG_3(T_2AG_3)_3$

Cation	ΔH (kcal/mol)	ΔS (cal/mol deg)	ΔG_{37} (kcal/mol)	T_m (°C)
100 mM Na^+ [a]	-72.7 ± 1.1	-192 ± 3.2	-13.2 ± 0.2	63.7
100 mM K^+ [a]	-77.5 ± 1.5	-202 ± 4.2	-14.8 ± 0.2	69.3
10 mM Mg^{2+} [a]	-34.7 ± 0.8	-90.9 ± 2.6	-6.5 ± 1.1	36.0
1 mM Sp^{3+} [a]	-66.0 ± 0.7	-179 ± 2.1	-10.5 ± 1.0	54.7
1 mM Sp^{4+} [a]	-57.4 ± 0.5	-153 ± 1.5	-9.9 ± 0.7	53.4
100 mM Na^+ [b]	-63.2 ± 0.4	-166 ± 1.1	-11.6 ± 0.5	61.6

[a]pH value of buffer is adjusted to 7.0.
[b]pH value of buffer is adjusted to 5.5.

Table 2
Thermodynamic parameters of equimolar mixture of $dG_3(T_2AG_3)_3/d(C_3TA_2)_3C_3$ at pH 7.0

	ΔH_{VH}[a] (kcal/mol)	ΔH_{VH}[b] (kcal/mol)	ΔH_{CAL} (kcal/mol)	T_m[c] (°C)	ΔG_{37}[a] (kcal/mol)
100 mM Na^+	−104 ± 5.7	−127 ± 6.4	−52.1	71.5	−17.0 ± 1.1
10 mM Mg^{2+}	−223 ± 6.6	−120 ± 5.4	−79.1	74.4	−30.5 ± 0.9

[a]Calculated using T_m^{-1} vs. ln (Ct/4) plots.
[b]Calculated using non-linear least-squares fitting method.
[c]The melting temperature at the total concentration of 100 μM.

3.3. Structural transition competition in $dG_3(T_2AG_3)_3/d(C_3TA_2)_3C_3$

Thermodynamic parameters of $dG_3(T_2AG_3)_3/d(C_3TA_2)_3C_3$ (equimolar ratio) in 100 mM Na^+ and 10 mM Mg^{2+} at pH 7.0 were calculated using the UV melting curves [23,24] and are listed in Table 2. The large disparities between van 't Hoff enthalpy, ΔH_{VH}, and calorimetric enthalpy, ΔH_{CAL}, reflect that it was a non-two-state transition system in either Na^+ or Mg^{2+} buffer.

CD spectra of $dG_3(T_2AG_3)_3/d(C_3TA_2)_3C_3$ had a peak of 265 nm at pH 7.0 with either Na^+ (as shown in Fig. 4), K^+ or Mg^{2+} (data not shown), which is the characteristic of A-form DNA duplex [25]. However, a shoulder band near 287 nm suggested certain structural information different from the usual duplex. The intensity of the shoulder band increased as the pH value decreased. The shoulder band in the double-stranded system probably reflected the existence of an alternative structure to the WC duplex.

Next, we studied the temperature dependence of CD spectra for the double strand. At neutral conditions, there were two isosbestic points in CD profiles with either Na^+ (data not shown) or Mg^{2+} (as shown in Fig. 5A). The intersected points were near 227 and 249 nm with Mg^{2+} at pH 7.0, while in neutral Na^+ buffer they turned out to be near 224 and 250 nm. As the pH value of the Na^+ buffer decreased to 5.5, there appeared three isosbestic points located at 209, 228 and 250 nm, respectively (as shown in Fig. 5B). The third intersected point at 209 nm should be due to the high stability of the I-motif $d(C_3TA_2)_3C_3$ at acidic pH. These multi-isosbestic-point spectra are obvious evidences for the formation of intermediates [26].

The native PAGE images clearly showed that there existed two bands even in the equimolar mixture of $dG_3(T_2AG_3)_3$ and $d(C_3TA_2)_3C_3$ at the neutral Na^+ buffer (as shown in Fig. 3A). The slower band was relevant to the duplex and the faster one to the quadruplex. In neutral Mg^{2+} buffer there only appeared a tiny shadow area besides the duplex band in the equimolar double-stranded system, because Mg^{2+} has the effect of stabilizing the duplex [27] but destabilizing the G-quadruplex (as listed in Tables 1 and 2).

Comparison of DSC results between the single strand and the double strand also confirmed the existence of the quadruplex in the double-stranded system. Fig. 6 indicates that there exist two bands in the excess heat capacity profile of the double-stranded system with Mg^{2+}, of which the strong band is relative to the duplex while the weak one corresponds to the less stable G-quadruplex. However, in Na^{2+} buffer the excess heat capacity profile of the double strand showed a single band with a broad base and a narrow peak (data not shown), because the transition temperature of the quadruplex (64°C) was very close to that of the duplex (69°C). All these results suggest that the cation species and pH values may adjust the competitive equlibria between quadruplexes and duplexes.

According to the experimental results, a structure competitive mechanism was put forward for the double-stranded $dG_3(T_2AG_3)_3/d(C_3TA_2)_3C_3$ system (as shown in Scheme 1). At acidic sodium buffer, both G-quadruplex of $dG_3(T_2AG_3)_3$

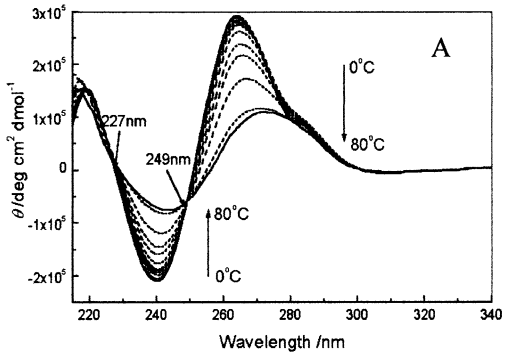

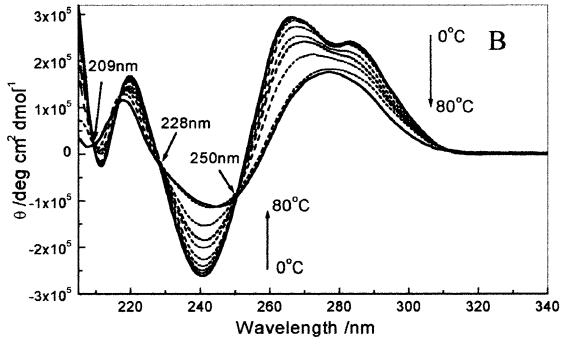

Fig. 5. CD spectra of $dG_3(T_2AG_3)_3/d(C_3TA_2)_3C_3$ (1:1) at selected temperatures in 10 mM Mg^{2+} at pH 7.0 (A) and 100 mM Na^+ at pH 5.5 (B), respectively.

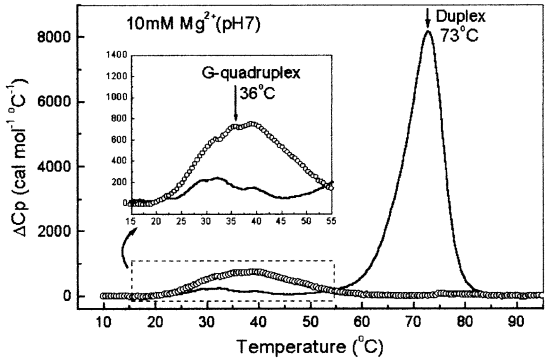

Fig. 6. DSC comparison of $dG_3(T_2AG_3)_3$ and $dG_3(T_2AG_3)_3/d(C_3TA_2)_3C_3$ in 10 mM Mg^{2+} buffer (50 mM MES, pH 7.0).

and I-motif of $d(C_3TA_2)_3C_3$ are thermodynamically stable, consequently there appears a clear structure competition against the WC duplex. However, at neutral pH, especially with Mg^{2+} that can destabilize the G-quadruplex, the equilibria favor the formation of the duplex. Our preliminary kinetic researches also confirmed great influences of cation species and pH values on the rate of duplex formation.

4. Conclusion

The thermodynamic properties of G/C-rich oligomers investigated in this study reflected that the cation species and pH values have dramatic effects on the structure competitive equilibria of the G-quadruplex, I-motif and the WC duplex. Our results reinforce the probability to modulate the tertiary structures of nucleic acids in vivo, which will be very useful for the design of structure-specific oligonucleotides for antigen chemotherapy and in situ cellular inhibition of telomerase etc.

Acknowledgements: This work was supported in part by Grants-in-Aids from the Ministry of Education, Science, Sports and Culture, Japan to N.S.

References

[1] Blackburn, E.H. (1994) Cell 77, 621–623.
[2] Marx, J. (1994) Science 265, 1656–1658.
[3] Mariappan, S.V., Catasti, P., Chen, X., Ratliff, R., Moyzis, R.K., Bradbury, E.M. and Gupta, G. (1996) Nucleic Acids Res. 24, 784–792.
[4] Williamson, J.R. (1994) Annu. Rev. Biophys. Biomol. Struct. 23, 703–730.
[5] Venczel, E.A. and Sen, S. (1996) J. Mol. Biol. 257, 219–224.
[6] Kang, C., Berger, I., Lockshin, C., Ratlife, R., Moyzis, R. and Rich, A. (1995) Proc. Natl. Acad. Sci. USA 92, 3874–3878.
[7] Mergny, J. (1999) Biochemistry 38, 1573–1581.
[8] Nonin-Lecomte, S. and Leroy, J. (2001) J. Mol. Biol. 309, 491–506.
[9] Matsugami, A., Ouhashi, K., Kanagawa, M., Liu, H., Kanagawa, S., Uesugi, S. and Katahira, M. (2001) J. Mol. Biol. 313, 255–269.
[10] Miyoshi, D., Nakao, A., Toda, T. and Sugimoto, N. (2001) FEBS Lett. 496, 128–133.
[11] Simonsson, T. (2001) Biol. Chem. 382, 621–628.
[12] Bolten, M., Niermann, M. and Eimer, W. (1999) Biochemistry 38, 12416–12423.
[13] Sugimoto, N., Toda, T. and Ohmichi, T. (1998) Chem. Commun. 1533–1534.
[14] Miura, T. and Thomas, G. (1994) Biochemistry 33, 7848–7856.
[15] Deng, H. and Braunlin, W. (1995) Biopolymers 35, 677–681.
[16] Manzini, G., Yathindra, N. and Xodo, L. (1994) Nucleic Acids Res. 22, 4634–4640.
[17] Richards, E.G. (1975) in: Handbook of Biochemistry and Molecular Biology: Nucleic Acids (Fasman, G.D., Ed.) 3rd Edn., Vol.1, pp. 596–603, CRC Press, Cleveland, OH.
[18] Balagurumoorthy, P., Brahmachari, S., Mohanty, D., Bansal, M. and Sasisekharan, V. (1992) Nucleic Acids Res. 20, 4061–4067.
[19] Henderson Jr., E., Hardin, C., Walk, S.K., Tinoco, I. and Blackburn, E.H. (1987) Cell 51, 899–908.
[20] Marathias, M.V. and Bolton, H.P. (1999) Biochemistry 38, 4355–4364.
[21] Balagurumoorthy, P. and Brahmachari, S. (1994) J. Biol. Chem. 269, 21858–21869.
[22] Leroy, J.L., Gueron, M., Mergny, J.L. and Helene, C. (1994) Nucleic Acids Res. 22, 1600–1606.
[23] Wu, P. and Sugimoto, N. (2000) Nucleic Acids Res. 28, 4762–4768.
[24] Nakano, S., Fujimoto, M., Hara, H. and Sugimoto, N. (1999) Nucleic Acids Res. 27, 2957–2965.
[25] Sugimoto, N. and Sato, N. (1999) Rep. Progr. Polymer Phys. Jpn. 42, 569–572.
[26] Xiang, H., Dong, J., Carey, P.R. and Dunaway, M.D. (1999) Biochemistry 38, 4207–4213.
[27] Hou, M., Lin, S., Yuann, J., Lin, W., Wang, A. and Kan, L. (2001) Nucleic Acids Res. 29, 5121–5128.